Width of a ferrofluid finger: Hysteresis and a double energy minimum

Narelle J. Hillier and David P. Jackson

Department of Physics and Astronomy, Dickinson College, Carlisle, Pennsylvania 17013, USA

We study a ferrofluid in a horizontal Hele-Shaw geometry subjected to a vertical magnetic field. Specifically, we calculate the energy of a single ferrofluid finger using an idealized model for the finger. By minimizing this energy, we find the preferred finger width as a function of the applied field. Our model predicts a first order transition as the fluid abruptly transforms from a circular drop to a finite finger. This behavior arises because of a double energy minimum that yields two different stable configurations for the system. Interestingly, this system exhibits hysteresis as the circle-to-finger (increasing field) transition occurs at a different applied field than the finger-to-circle (decreasing field) transition. We carry out a simple experiment and observe good overall agreement with the theoretical predictions.

I. INTRODUCTION

Ferrofluids are magnetic liquids composed of minute ($\sim$10 nm) single-domain particles coated with a molecular surfactant and suspended in a carrier liquid [1]. These fluids behave superparamagnetically and are dramatically influenced by external magnetic fields. When no external magnetic field is present, these liquids behave like any other liquid. However, in the presence of an external magnetic field, the microscopic dipoles in the liquid align with the applied field. This magnetization of the fluid leads to a number of interesting pattern forming situations including the so-called Rosensweig (normal field) instability, a magnetic Rayleigh-Taylor instability, and the stabilization of fluid cylinders [2–4].

One of these instabilities occurs when a ferrofluid drop is trapped between two closely spaced glass plates (a Hele-Shaw cell) and subjected to a perpendicular magnetic field (Fig. 1). In this situation, the traditional Saffman-Taylor instability [5] is augmented by magnetic interactions and the ferrofluid can evolve into a complex, mazelike structure [6–9]. One way this so-called labyrinthine structure can be formed is to slowly increase the strength of the applied magnetic field so that the ferrofluid drop first forms a fingerlike structure. As the strength of the field increases, this finger grows longer and thinner, meandering around the cell until it is no longer recognizable as a single finger.

Although the width of a labyrinthine finger was originally calculated for a stripe configuration over twenty years ago [10], a mistake was recently found in this result and the corrected calculations do not appear to agree as closely with experiments as the earlier calculations [11]. This surprising turn of events led us to consider analyzing a slightly simpler system. In this study, we investigate the width of a ferrofluid finger *before* it begins meandering into the more complex labyrinthine pattern. An example of such a finger is shown in Fig. 2. The basic approach is to calculate the total energy of a ferrofluid finger in a Hele-Shaw geometry, and then minimize this energy as a function of the finger width. As we will show, this procedure leads to a double minimum in the energy that gives rise to two stable configurations and hysteresis in this system.

II. ENERGY OF A FERROMAGNETIC FINGER

In general, the total energy of a ferrofluid system consists of three components: gravitational, surface, and magnetic. For a ferrofluid in a horizontal Hele-Shaw cell, the gravitational energy is constant and can be neglected. This leaves only the surface and magnetic energies. Assuming that the interface between the ferrofluid and the outer fluid is vertical, the surface energy is given by

$$E_s = \sigma h P, \tag{1}$$

where σ is the surface tension, h is the plate spacing in the Hele-Shaw cell, and P is the perimeter of the domain. In order to determine the field energy, we assume that the magnetization of a ferrofluid in a uniform magnetic field is constant. The magnetic energy is then given by [8]

$$E_m = \frac{\mu_0 h M^2}{2} \left[A - \frac{1}{2\pi} \oint ds \oint ds' \hat{\mathbf{t}} \cdot \hat{\mathbf{t}}' \Phi(R/h) \right], \tag{2}$$

where μ_0 is the permeability of free space, M is the magnetization of the ferrofluid, and A is the area of the domain as seen from above. The integration is carried out over the perimeter of the domain with s and s' representing arc-length coordinates along the contour of the domain, and $\hat{\mathbf{t}}$ and $\hat{\mathbf{t}}'$ are unit tangent vectors at s and s', respectively (Fig. 3). The
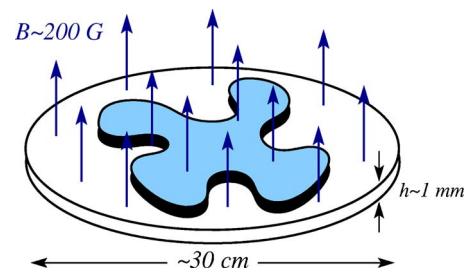

FIG. 1. (Color online) Schematic diagram of the geometry of the ferrofluid system. A ferrofluid droplet is trapped between two closely spaced horizontal glass plates and subjected to a vertical magnetic field. The resulting competition between surface tension and the destabilizing magnetic pressure leads to a fingering instability that can result in a complex labyrinthine pattern.

FIG. 2. Photographs of a ferrofluid droplet in a Hele-Shaw cell with no magnetic field (top) and with a perpendicular external magnetic field (bottom).

distance between s and s' is given by $R=|\mathbf{r}-\mathbf{r}'|$ and $\Phi(\xi)$ $=\sinh^{-1}(1/\xi)-\sqrt{1+\xi^2}+\xi$ is a coupling strength that arises from integration over the height of the domain. Because a uniformly magnetized domain is equivalent to a current flowing around the exterior of the domain, the integral portion of Eq. (2) can be viewed as a current-current interaction. In this sense, the evolution of a ferrofluid droplet in a Hele-Shaw cell is equivalent to the motion of a tense current ribbon.

In order to calculate and minimize the total energy of this system, it is first necessary to develop an idealized model for the shape of a ferrofluid finger. As can be seen in Fig. 2 a real ferrofluid finger has a fairly constant finger width but slightly bulbous ends. To simplify the analysis somewhat, we take the finger to be perfectly straight with a constant width and having ends consisting of half circles, as shown in Fig. 3. We partition the perimeter of the finger into four segments consisting of two straight lines of length $2L$ and two semicircles of radius w; these segments are numbered 1–4 beginning with the right semicircle and moving counterclockwise. Note that because the volume of the ferrofluid is fixed, L and w are not independent quantities. If R_0 is the radius of the initial droplet then

$$L=\frac{\pi}{4w}(R_0^2-w^2). \qquad (3)$$

Thus as the finger grows longer, it necessarily becomes thinner.

Using this parametrization, the double integral in Eq. (2) can be broken down into 16 separate terms, each of the four segments (labeled i) being paired with every other segment (labeled j). The magnetic energy can therefore be written as

$$E_m=\frac{\mu_0hM^2}{2}\left(A-\frac{1}{2\pi}\sum_{i,j=1}^{4}I_{ij}\right), \qquad (4)$$

where I_{ij} represents the integral contribution corresponding to the ith and jth segments. For example,

$$I_{12}=\int\int d\mathbf{r}_1\cdot d\mathbf{r}_2\Phi(R_{12}/h)$$
$$=w\int_{-L}^{L}dx\int_{-\pi/2}^{\pi/2}d\theta\sin(\theta)\Phi(R_{12}/h), \qquad (5)$$

where $R_{ij}=\sqrt{(x_i-x_j)^2+(y_i-y_j)^2}$ gives the separation distance between points on the ith and jth segments. For $i=1$ and $j=2$, this separation distance is

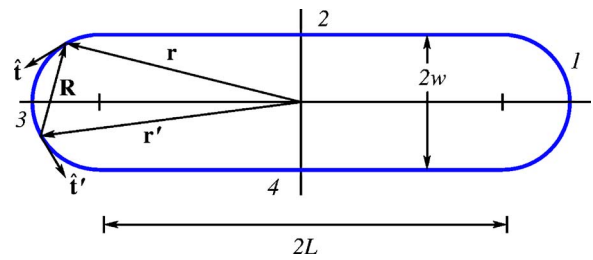$$R_{12}=\sqrt{(x-L-w\cos\theta)^2+w^2(1-\sin\theta)^2}. \qquad (6)$$

FIG. 3. (Color online) A model of an idealized ferrofluid finger consisting of two parallel line segments of length $2L$ and two semicircles of radius w; these segments are numbered 1–4. Note that this model does not account for the bulbous tips observed in a real ferrofluid finger as seen in Fig. 2.

Because of the symmetry present in our model, we immediately note that $I_{11}=I_{33}$, $I_{22}=I_{44}$, and $I_{ij}=I_{ji}$ when $i\neq j$. This reduces the number of integrals from 16 down to 8. Referring back to Fig. 3, we also observe that $I_{12}=I_{14}=I_{23}=I_{34}$, since each integral is comprised of one semicircle and one straight line segment. As a result, we end up with only five independent integrals to consider. Equation (4) can therefore be written

$$E_m=\frac{\mu_0h\pi R_0^2M^2}{2}\left(1-\frac{2}{\pi^2}\sum_{i=1}^{5}J_i\right), \qquad (7)$$

where J_i represents dimensionless integrals defined in the Appendix.

We are now in a position to write the total energy of the ferrofluid finger. It is convenient to write this energy in dimensionless form as $\widetilde{E}=E/\sigma R_0^2$. Noting that the perimeter of a finger is $P=4L+2\pi w$, we combine Eqs. (1), (3), and (7) to get

$$\widetilde{E}=\frac{2\pi}{p}\left(\frac{1+\widetilde{w}^2}{\widetilde{w}}\right)+N_B\pi^2\left(1-\frac{1}{\pi^2}\sum_{i=1}^{5}J_i(\widetilde{w})\right), \qquad (8)$$

where $\widetilde{w}=w/R_0$, $p=2R_0/h$ is the aspect ratio, and N_B is the (dimensionless) magnetic Bond number defined by

$$N_B=\frac{\mu_0M^2h}{2\pi\sigma}. \qquad (9)$$

This magnetic Bond number gives the ratio of the magnetic energy to the surface energy. Since the surface tension remains constant for our system, the Bond number conveniently serves as an indicator of the strength of the applied magnetic field.

Equation (8) represents one of the central results of this paper. For a fixed plate spacing and magnetic field value, this equation gives the total (dimensionless) energy of a ferrofluid finger in an applied magnetic field in terms of the single parameter $\widetilde{w}$. This parameter $\widetilde{w}=w/R_0=2w/2R_0$ is simply the width of the finger scaled by the initial diameter of the circle. Thus a value of $\widetilde{w}=1$ corresponds to a circle and as $\widetilde{w}$ decreases, the finger becomes longer and thinner.

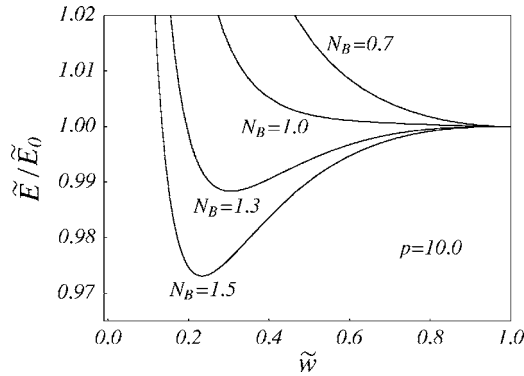The energy of a circular ferrofluid domain has been previously calculated and is given by [8]

FIG. 4. A plot of (scaled) energy as a function of finger width for a fixed aspect ratio, $p=10$, and four different magnetic Bond numbers calculated using Eq. (8) scaled by Eq. (10). The preferred finger width, denoted by the location of the minimum, decreases as the applied field increases.

$$\tilde{E}_0 = \frac{4\pi}{p} + N_B \pi^2$$
$$\times \left(1 + \frac{4pN_B}{3\pi}\{1 - k^{-3}[(2k^2 - 1)E(k) + (1 - k^2)K(k)]\}\right),$$
(10)

where E and K are complete elliptic integrals of the first and second kind, respectively, and $k^2 \equiv p^2/(1+p^2)$. Of course, Eq. (8) with $\tilde{w}=1$ (a circle) should be equivalent to Eq. (10) and indeed, numerical computations show that these two equations give identical results.

To facilitate our understanding of Eq. (8), it is convenient to scale the energy of a finger by Eq. (10), the energy of a circle. This allows us to plot multiple curves on the same graph for easy comparison. Figure 4 shows a graph of the total energy as a function of finger width for a fixed aspect ratio, $p=10$, and for four magnetic Bond numbers, $N_B=0.7$, 1.0, 1.3, and 1.5. The location of each minimum corresponds to the preferred finger width. As can be seen in Fig. 4, the energy is minimized when $\tilde{w}=1$ (a circle) for small magnetic fields (low N_B). For $p=10$, an energy minimum corresponding to a finger first appears at $N_B \approx 1.049$ and as the field increases, the energy minimum moves toward $\tilde{w}=0$ as the preferred finger width decreases.

III. A DOUBLE MINIMUM AND HYSTERESIS

As seen in Fig. 4, the preferred finger width decreases as the applied field increases. Thus if we can find the energy minima from Eq. (8), we can plot the finger width as a function of applied field. Interestingly, while performing these calculations we discovered a curious feature of this system. Near the transition from a circular domain to a finger, we find that the energy graph has a double well behavior. That is, our model predicts that there are two stable configurations for a range of applied field values. Figure 5 demonstrates this behavior for $p=10$ and $N_B=1.0617$. It is worth noting that the energy barrier in this figure is quite small.

One immediate consequence of this behavior is that the preferred finger width first appears with a finite value. That
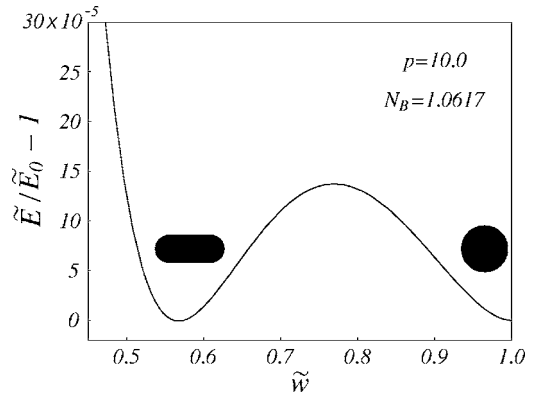

FIG. 5. Near the transition from circle to finger, our model predicts two stable states, represented by a double minimum in the plot of energy vs finger width. Here, for $p=10$ and $N_B=1.0617$, the energies of each state are approximately the same even though the shapes are quite different.

is, the system will undergo a first-order transition as it abruptly changes from a circle to a finite finger. This happens because there is a barrier that separates the two energy minima. Unless this barrier is extremely small, the system can stay "trapped" in one of these local minima even if the second minimum corresponds to a lower energy state. Therefore as the magnetic field is increased, the system should stay trapped in the circular state until the barrier disappears. Conversely, once a finger has formed and the magnetic field is decreased, the system should stay trapped in the finger state until the barrier disappears. These two transitions will occur for different magnetic field values. Thus the system should exhibit hysteresis. Using a similar approach (but a different theoretical model), de Koker and McConnell report seeing the same behavior in a lipid monolayer system [12]. Of course, if the energy barrier is small enough, it may be essentially nonexistent. In this case, we should only see a single transition that takes place when the two energy minima are approximately equal.

Surprisingly, although the size of the energy barrier becomes smaller and smaller as the external field is increased, it never completely disappears. Consequently, some method is needed to determine an approximate cutoff for which the depth of the local minimum at $\tilde{w}=1$ is insignificant compared to the depth of the local minimum of the finger. We choose this transition to be when the depth of the finger minimum is 100 times greater than the depth of the circle minimum. For $p=10$, this occurs at $N_B \approx 1.128$. Using this prescription, we can then determine the preferred finger width as a function of applied field. Figure 6 shows a graph of the preferred finger width as a function of the magnetic Bond number. The vertical dotted lines denote the transitions that occur as the system changes from a circle to finger (right transition) and from finger to a circle (left transition). Within the region of the figure enclosed by these transitions, there are two stable states. Thus it might be possible to prod the ferrofluid so that it changes from one stable configuration to the other.

A comparison of preferred finger widths for different aspect ratios reveals that larger droplets form fingers at smaller
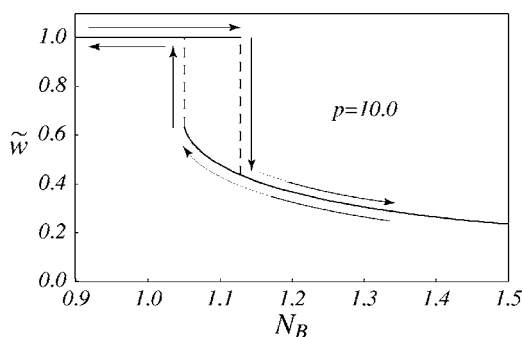
FIG. 6. Finger width as a function of magnetic Bond number. Because of the double minimum in the energy, this system exhibits hysteresis and the transitions are first order. As N_B increases, the circle should remain stable until reaching the right discontinuity. At this point the circle will transition to a finite finger and as the Bond number increases, the finger will decrease in width. As the Bond number decreases, the finger should remain stable until reaching the left discontinuity.

field values (Fig. 7). To make this figure easier to understand, we did not include the two separate transitions as shown in Fig. 6; instead, we include only a single transition chosen when the two local minima have approximately the same value. This figure also shows that for a specific Bond number, a larger aspect ratio has a smaller (scaled) finger width. Interestingly, the initial finger width remains approximately the same even as the aspect ratio is changed.

IV. EXPERIMENTAL RESULTS

To test our theoretical predictions, we performed a series of simple experiments using a Hele-Shaw cell consisting of two $30 \times 30 \times 0.6$ cm glass plates separated by a 1-mm spacer. The top plate has two small holes on opposite corners to allow injection of the ferrofluid. The magnetic field is produced using two large coils ($N \approx 660$, $R_{\mathrm{avg}} = 32$ cm) arranged in a Helmholtz configuration and connected to a power supply capable of delivering 18 A at 150 V dc. The result is a magnetic field of up to $B = 0.034$ T that is constant
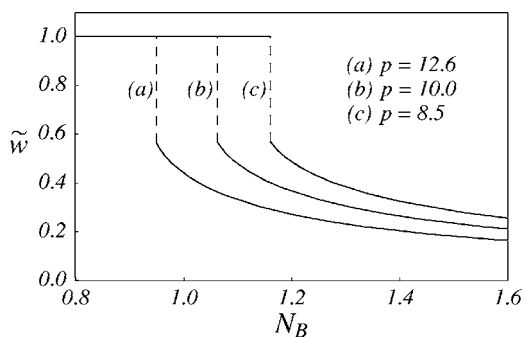

FIG. 7. Finger width curves for three different aspect ratios. At larger aspect ratios, the droplet becomes unstable for smaller Bond numbers and has a smaller (scaled) finger width for a given Bond number. For simplicity, the transition from circle to finger is marked by the single Bond number for which the two energy minima are approximately equal.

FIG. 8. Experimental results of a ferrofluid in a Hele-Shaw cell. As the magnetic field strength is increased, the finger becomes longer and thinner. The top image has no applied field and the second image from the top represents the first stable finger we found. This rather dramatic change is consistent with the first-order transition predicted in Fig. 6.

to within 1% over the central region of the Hele-Shaw cell [13]. Images of the ferrofluid are obtained by mounting a charge-coupled device camera (1280×1024 resolution) about 50 cm above the Hele-Shaw cell. The Hele-Shaw cell is backlit using a fluorescent light and the bottom piece of glass is frosted on the outside to diffuse the light and produce a relatively uniform intensity over the entire cell. This setup results in high contrast images that are easy to analyze. The entire system is computer controlled [14], allowing us to alter the voltage from the power supply, measure the actual current flowing in the circuit, and obtain images from the camera as desired.

The experimental procedure is as follows. We increase the applied magnetic field in small steps and take pictures of the ferrofluid after it has come to rest. Unfortunately, the ferrofluid tends to stick to the glass plates which makes it very difficult to obtain reproducible data. To try to eliminate this problem, we begin by thoroughly cleaning the glass plates before constructing the Hele-Shaw cell. Next, we insert a 0.25% solution of Tween-80 (Polyoxyethylenesorbitan monooleate) and distilled water into the cell. After letting it sit for a few days, we flush the cell with distilled water and repeat the process. Just prior to running an experiment, we inject the immiscible ferrofluid directly into the water/Tween mixture. We then use a small hand magnet to move the ferrofluid around inside the Hele-Shaw cell. We use a mineral-oil based ferrofluid (EFH1) manufactured by FerroTec Corporation [15]. This ferrofluid has an initial susceptibility of $\chi_i = 1.70$ and a saturation magnetization of $\mu_0 M_s = 0.040$ T.

After the ferrofluid is in the Hele-Shaw cell, we begin increasing the magnetic field. At each magnetic field value, we gently prod the ferrofluid drop with a small hand magnet and watch to see if it relaxes back to a circle. At some point, the ferrofluid grows into a finite finger. When the ferrofluid appears to stop moving, we take a picture and then proceed with another measurement. Figure 8 shows a few of these images.

Because the ferrofluid has a tendency to stick to the glass plates, we took multiple data points at each magnetic field value. In each case, we would approach the field value from below and from above so that the ferrofluid would be growing in one case and shrinking in the other case. Thus if stick-
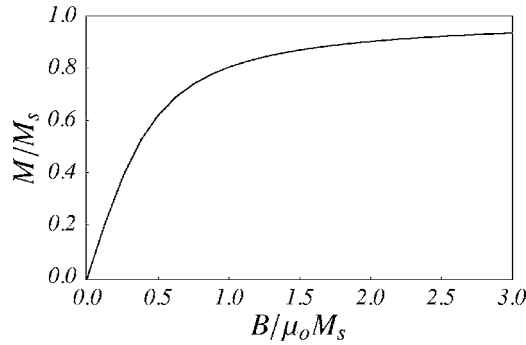
FIG. 9. Langevin magnetization curve for our ferrofluid as calculated from Eq. (11). Note that as the magnetic field increases, the magnetization of the ferrofluid begins to saturate.
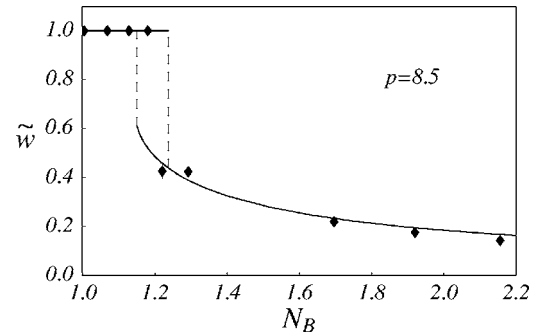

FIG. 10. A comparison of experimental results (diamonds) and the theoretical prediction for $p=8.5$. As predicted, the finger width drops rather suddenly at a particular Bond number and then decreases more slowly as the Bond number increases.

ing is a problem, we would expect a growing finger to be slightly shorter and fatter than a shrinking finger. We found very little difference between the growing and shrinking fingers indicating that sticking was not a major problem in the experiment.

In order to compare these experimental images with our theoretical predictions, it is necessary to determine the magnetization and surface tension of the ferrofluid as required by Eq. (9). For the magnetization, we assume that the ferrofluid obeys a superparamagnetic magnetization law as given by the Langevin equation [1]

$$M = M_s \left(\coth \alpha - \frac{1}{\alpha} \right), \tag{11}$$

where $\alpha = 3\chi_i B/\mu_0 M_s$. Figure 9 shows the behavior of this magnetization law for the EFH1 ferrofluid.

In addition to the ferrofluid magnetization, we need to know the surface tension between the ferrofluid and the water and Tween mixture in the Hele-Shaw cell. For a circular ferrofluid drop in a Hele-Shaw cell, the point of initial instability can be calculated analytically for small perturbations assuming the boundary of the drop is given (in polar coordinates) by $r(\theta) = R_0(1 + \epsilon \cos n\theta)$, where n is the (integer) mode number and $\epsilon \ll 1$ is the magnitude of the perturbation. For our situation, we are interested in the so-called elliptical instability ($n=2$), which has a critical Bond number given in terms of complete elliptic integrals by [7]

$$N_B^{cr} = \frac{9k(1-k^2)}{k^3(1-k^2)(8-3k^2)K(k) + (7k^2-8)E(k)}, \tag{12}$$

where as before, $k^2 = p^2/(1+p^2)$. Thus given a particular aspect ratio p, the critical Bond number at which a circular droplet is unstable to the elliptic instability is given by Eq. (12).

In our experiment, we find that a droplet with aspect ratio $p=8.5$ becomes unstable at a magnetic field value of $B=0.011$ T. Meanwhile, Eq. (12) gives $N_B^{cr}=1.16$ for the same aspect ratio. Using these values along with Eqs. (9) and (11), we calculate the surface tension to be $\sigma=0.030$ N/m.

The final step in our analysis is to determine the finger width from the raw image data. As pointed out earlier, the experimental fingers do not have a perfectly uniform finger width. This is particularly true for shorter fingers that have a "dog bone" type shape (see Fig. 8). Therefore the "width" of such a shape is not well defined. We use the Heywood circularity factor (F) to determine the width of the fingers. This factor gives the ratio of the perimeter of a domain to the circumference of a circle with the same area. Since the ferrofluid maintains a constant area while it evolves, this is an appropriate technique for determining the finger width. Beginning with the perimeter of our model finger (see Fig. 3), the scaled finger width can be calculated from

$$\widetilde{w} = w/R_0 = F - \sqrt{F^2 - 1}. \tag{13}$$

Figure 10 compares the experimental data to the prediction based on the simple finger model presented in this paper. Each data point is an average of four separate measurements, two in which the magnetic field was approached from below (growing finger) and two in which the field was approached from above (shrinking finger). Error bars denote the maximum and minimum finger width for each set of measurements and are only included when they extend beyond the size of the data point.

As can be seen in Fig. 10, the data shows good agreement with the theoretical predictions, even near the transition points. Thus our data support the prediction that the circle to finger transition is first order. However, we did not observe evidence of two stable configurations. In fact, a close inspection of Fig. 10 shows that there appears to be a single transition somewhere between the two predicted transitions. This suggests that the energy barrier is so small that it is effectively nonexistent. In this case, we would expect to observe a single transition that takes place when the two energy minima have equal values as shown in Fig. 7. As discussed earlier, this is not completely surprising based on the size of the energy barrier (note the vertical scale in Fig. 5).

To estimate our ability to measure the double minimum behavior, we use Eq. (8) to calculate the height of the energy barrier shown in Fig. 5 to be $\Delta \widetilde{E} \approx 1.3 \times 10^{-3}$. Then, using our experimental data in Fig. 10 [and Eq. (8) again], we see that it is relatively easy to distinguish energy differences of $\Delta \widetilde{E} \approx 1.4$. In fact, we could probably measure energy differences of $\Delta \widetilde{E} \approx 0.1$ without too much difficulty. Unfortu-

nately, it seems unlikely that we have the sensitivity to investigate the energy barrier with our current setup.

V. CONCLUSION

Using a simplified model for a ferrofluid finger, we have calculated the energy of a ferrofluid finger in a Hele-Shaw cell subjected to an external magnetic field. By using an energy minimization procedure, we determined the preferred finger width as a function of magnetic field. Our calculations show that the ferrofluid undergoes a first-order transition as it abruptly changes from a circle to a finite finger at a particular magnetic field value. Further analysis reveals that this system has two energetically stable configurations over a range of applied fields. This double minimum behavior provides the system with two stable evolutionary paths as the magnetic field is increased and decreased. Because there is an energy barrier between these two states, the system will remain in one state until the conditions are favorable for a discontinuous jump to the other state. Thus the system exhibits the behavior of a subcritical pitchfork bifurcation with the associated hysteresis that is common in such a system.

An experiment was performed to probe these findings and the results shows excellent agreement with the theoretical predictions. The ferrofluid droplet was observed to make a discontinuous transition from a circle to a finger and the finger width continued to decrease in accordance with our model as the magnetic field was increased. However, we did not observe hysteresis and therefore cannot confirm the existence of two simultaneously stable configurations. Unfortunately, our estimates show that it is unlikely we will be able to probe this behavior with our current experimental setup.

As previously mentioned, the finger model we have used in this paper does not take into account the bulbous tips of a real ferrofluid finger. This means a real ferrofluid evolution does not occur exactly as in our model. The most pronounced difference between our model and a real ferrofluid finger occurs very close to the transition from circle to finger; this is when the ferrofluid has a dog bone shape. Thus while our model can accurately predict the shape of a ferrofluid finger well beyond the transition region, we remain cautious about using this model near the transition region.

Because an actual ferrofluid finger differs from our model, we should mention that it is certainly possible that the ferrofluid evolves in such a way that the energy diagram does *not* exhibit a double minimum behavior (although it seems almost certain that the transition is first order in nature). Nevertheless, previous theoretical work on the shape transitions of lipid monolayers produced almost identical qualitative results to what we present here even though they used a completely different model for the shape of a finger (the so-called ovals of Cassini) [12]. Therefore the theoretical evidence certainly supports the notion of a double energy minimum, even if we are unable to observe it experimentally.

ACKNOWLEDGMENTS

APPENDIX: ENERGY INTEGRALS

Our finger model consists of two straight lines and two semicircles as represented in Fig. 3. Since the magnetic energy, Eq. (2), involves a double integral, it is necessary to integrate twice around the contour of the finger. The four segments thus lead to 16 individual integrals I_{ij}, where i and j are indices referring to the four different segments that make up the contour. As discussed in Sec. II, symmetry reduces the number of independent integrals from 16 down to 5. These five integrals J_i are given by

$$J_1 = I_{11}/R_0{}^2,$$

$$J_2 = 4I_{12}/R_0{}^2,$$

$$J_3 = I_{13}/R_0{}^2,$$

$$J_4 = I_{22}/R_0{}^2,$$

$$J_5 = I_{24}/R_0{}^2. \tag{A1}$$

As an example, the integral J_2 is given by

$$J_2 = 4\widetilde{w} \int_{-\widetilde{L}(\widetilde{w})}^{\widetilde{L}(\widetilde{w})} d\widetilde{x} \int_{-\pi/2}^{\pi/2} d\theta \sin(\theta)\Phi(R_{12}/h), \tag{A2}$$

where $\widetilde{x}=x/R_0$, $\widetilde{L}=L/R_0$, $\widetilde{w}=w/R_0$, and

$$R_{12}/h = \frac{p}{2}\sqrt{(\widetilde{x} - \widetilde{L} - \widetilde{r}\cos\theta)^2 + \widetilde{w}^2(1 - \sin\theta)^2}. \tag{A3}$$

[1] R. E. Rosensweig, *Ferrohydrodynamics* (Cambridge University Press, Cambridge, U.K., 1985).

[2] M. D. Cowley and R. E. Rosensweig, J. Fluid Mech. **30**, 671 (1967).

[3] R. E. Zelazo and J. R. Melcher, J. Fluid Mech. **39**, 1 (1969).

[4] B. M. Berkovsky and V. Bashtovoi, IEEE Trans. Magn. **MAG-16**, 288 (1980).

[5] P. G. Saffman and G. I. Taylor, Proc. R. Soc. London, Ser. A **245**, 312 (1958).

[6] L. T. Romankiw, M. Slusarczak, and D. A. Thompson, IEEE Trans. Magn. **MAG-11**, 25 (1975).

[7] A. O. Tsebers and M. M. Maiorov, Magnetohydrodynamics

(N.Y.) **16**, 21 (1980).

[8] S. A. Langer, R. E. Goldstein, and D. P. Jackson, Phys. Rev. A **46**, 4894 (1992).

[9] G. Pacitto, C. Flament, J.-C. Bacri, and M. Widom, Phys. Rev. E **62**, 7941 (2000).

[10] R. E. Rosensweig, M. Zahn, and R. Shumovich, J. Magn. Magn. Mater. **39**, 127 (1983).

[11] J. Richardi, D. Ingert, and M. P. Pileni, J. Phys. Chem. B **106**, 1521 (2002).

[12] R. de Koker and H. M. McConnell, J. Phys. Chem. **97**, 13419 (1993).

[13] S. Robinson and T. Sparacio (unpublished).

[14] We use LabVIEW, available from National Instruments, Inc. (www.ni.com).

[15] EFH1 ferrofluid is widely available through a number of educational suppliers. See www.ferrotec.com for more information.